**Atmospheric
Measurement
Techniques
Discussions**

Relative drifts and stability of satellite and ground-based stratospheric ozone profiles at NDACC lidar stations

P. J. Nair[1], S. Godin-Beekmann[1], L. Froidevaux[2], L. E. Flynn[3], J. M. Zawodny[4], J. M. Russell III[5], A. Pazmiño[1], G. Ancellet[1], W. Steinbrecht[6], H. Claude[6], T. Leblanc[7], S. McDermid[7], J. A. E. van Gijsel[8], B. Johnson[9], A. Thomas[10], D. Hubert[11], J.-C. Lambert[11], and H. Nakane[12]

[1]LATMOS-IPSL, UMR8190, CNRS/INSU – UPMC Université Paris 06, Paris, France
[2]Jet Propulsion Laboratory, California Institute of Technology, Pasadena, California, USA
[3]National Oceanic and Atmospheric Administration, 5200 Auth Rd, Camp Springs, MD, USA
[4]Chemistry and Dynamics Branch, NASA Langley Research Center, Hampton, Virginia, USA
[5]Center for Atmospheric Sciences, Hampton University, Hampton, Virginia, USA
[6]Meteorologisches Observatorium, Deutscher Wetterdienst, Hohenpeißenberg, Germany
[7]Table Mountain Facility, Jet Propulsion Laboratory, Wrightwood, CA, USA
[8]Royal Netherlands Meteorological Institute, De Bilt, The Netherlands

Discussion Paper | Discussion Paper | Discussion Paper | Discussion Paper

AMTD

5, 471–516, 2012

Stability of ozone measurement systems

P. J. Nair et al.

Title Page

Abstract | Introduction

Conclusions | References

Tables | Figures

|◀ | ▶|

◀ | ▶

Back | Close

Full Screen / Esc

Printer-friendly Version

Interactive Discussion

[9]Climate Monitoring and Diagnostics Laboratory, National Oceanic and Atmospheric Administration, Boulder, USA
[10]National Institute of Water and Atmospheric Research, Lauder, Central Otago, New Zealand
[11]Belgium Institute for Space Aeronomy, (IASB-BIRA), Brussels, Belgium
[12]National Institute for Environmental Studies, Ibaraki 305, Japan

Correspondence to: P. J. Nair (gopalapi@aero.jussieu.fr)

Stability of ozone measurement systems

P. J. Nair et al.

Title Page

Abstract | Introduction

Conclusions | References

Tables | Figures

|◄ | ►|

◄ | ►

Back | Close

Full Screen / Esc

Printer-friendly Version

Interactive Discussion

Abstract

The long-term evolution of stratospheric ozone at different stations in the low and mid-latitudes is investigated. The analysis is performed by comparing the collocated profiles of ozone lidars, at the northern mid-latitudes (Meteorological Observatory Hohenpeißenberg, Haute-Provence Observatory, Tsukuba and Table Mountain Facility), tropics (Mauna Loa Observatory) and southern mid-latitudes (Lauder), with ozonesondes and space-borne sensors (SBUV(/2), SAGE II, HALOE, UARS MLS and Aura MLS), extracted around the stations. Relative differences are calculated to find biases and temporal drifts in the measurements. All measurement techniques show their best agreement with respect to the lidar at 20–40 km, where the differences are within ±3 % and drifts are less than ±0.3 % yr^{-1} at all stations. In addition, the stability of the long-term ozone observations (lidar, SBUV(/2), SAGE II and HALOE) is evaluated by the cross-comparison of each data set. In general, all lidars and SBUV(/2) exhibit near zero drifts and the comparison between SAGE II and HALOE shows larger, but insignificant drifts. The RMS of the drifts of lidar and SBUV(/2) is 0.22 and 0.27 % yr^{-1}, respectively. The average drifts of the long-term data sets, derived from various comparisons, are less than ±0.3 % yr^{-1} in 20–40 km at all stations. A combined time series of the relative differences between SAGE II, HALOE and Aura MLS with respect to lidar data at six sites is constructed, to obtain long-term data sets lasting up to 27 yr. The relative drifts derived from these combined data are very small, within ±0.2 % yr^{-1}.

1 Introduction

The discovery of Antarctic ozone hole (Farman et al., 1985) and the understanding of the negative impacts of ozone depleting substances (ODS) on the evolution of ozone layer led to the creation of international treaties (Vienna Convention, in 1985, Montreal Protocol, in 1987), which to a large extent, have phased out production and emission of harmful chlorofluorocarbons. The analysis of stratospheric ozone trends in the wake

of declines in the abundances of ODSs in the stratosphere are currently the focus of stratospheric ozone research. Statistical studies of ozone content in the upper stratosphere have revealed a strong decreasing trend until the mid-1990s and a levelling off after 1996, consistent with the decreasing trend in upper stratospheric HCl (Reinsel

5   et al., 2002; Newchurch et al., 2003; WMO, 2007; Jones et al., 2009; Steinbrecht et al., 2009b). A study by Steinbrecht et al. (2006) found upper stratospheric ozone trends of about -6, -4.5 and $-8\,\%\,\text{decade}^{-1}$ at northern mid-latitude, subtropics and southern mid-latitude stations, respectively before 1997. After 1997, changes in the trends by about 7, 7 and $11\,\%\,\text{decade}^{-1}$ were evaluated at the respective stations.

10 In the lower stratosphere too, studies have shown a negative trend until the mid-1990s and a positive trend afterwards at selected low and mid-latitude regions (Yang et al., 2006; Zanis et al., 2006). These studies suggest that the decrease in ozone depletion between 18 and 25 km is consistent with the reduction in stratospheric chlorine and bromine amounts, whereas below 18 km the increase in ozone is most likely driven

15 by changes in atmospheric transport. In a recent study, Dhomse et al. (2006) found that the rapid increase of northern hemispheric total ozone to a lesser extent is due to the effect of enhanced residual circulation and solar activity during the recent years, which is also confirmed in a study by Harris et al. (2008). Weatherhead and Anderson (2006) reported that an understanding of the ozone recovery to the pre-1980 levels is

20 possible only after differentiating the effects of transport, temperature, and solar cycle on observed ozone changes. Hence, an accurate evaluation of ozone trends and an understanding of the factors playing important roles in the increase or decrease of ozone are necessary to evaluate the efficiency of the Montreal Protocol for the preservation of the ozone layer. This evaluation depends largely on the quality and continuity

25 of the measurements used for the studies. Because instrument stability is essential to derive statistically significant ozone trends, a consistent evaluation of ozone observations is crucial for the estimation of trends and the prediction of ozone evolution in the future.

Stability of ozone measurement systems

P. J. Nair et al.

P. J. Nair et al.

The Network for the Detection of Atmospheric Composition Change (NDACC) is an international network set up in 1991. NDACC relies on worldwide measurement stations with various instruments designed initially for the simultaneous monitoring of atmospheric parameters involved in the ozone depletion issue. Recently, NDACC has broadened its scope with the monitoring of atmospheric composition in the free and upper troposphere and the mesosphere. One of the main goals of NDACC is the calibration and validation of space-based observations. For that purpose, a careful evaluation of the stability of NDACC ground-based measurements is necessary. In this context, a thorough analysis of 6 satellite and 2 ground-based ozone data sets was performed at one of the NDACC lidar stations, located at Haute-Provence Observatory (Nair et al., 2011).

The present work extends this study to other NDACC lidar stations located in the tropical and mid-latitude regions. We focus on NDACC lidar stations providing long-term and continuous ozone measurements, namely the northern mid-latitude stations of Meteorological Observatory Hohenpeißenberg (MOHp: 47.8° N, 11.02° E), Haute-Provence Observatory (OHP: 43.93° N, 5.71° E), Tsukuba (36° N, 140.01° E) and Table Mountain Facility (TMF: 34.5° N, 117.7° W), the tropical station of Mauna Loa Observatory (MLO: 19.5° N, 155.7° W) and the southern mid-latitude station of Lauder (45.03° S, 169.7° E). The data quality is checked by intercomparing different ozone observations at each station. Lidar profiles and ozonesonde data (if available nearby), as well as satellite profiles sampled near the stations are utilised for this. The ozonesonde observations at Tateno (36.06° N, 140.13° E) and Hilo (19.72° N, 155.07° W) are considered for the comparisons with other observations at Tsukuba and MLO, respectively. Space-borne data sets include those from Solar Backscatter UltraViolet (SBUV)(/2), Stratospheric Aerosol and Gas Experiment (SAGE) II, Halogen Occultation Experiment (HALOE) and Microwave Limb Sounder (MLS) on board the Upper Atmosphere Research Satellite (UARS) and Aura.

This article is organised in the following way: introduction is followed by the data description of lidar, ozonesondes and the satellite observations in Sect. 2. The

methodology used for the analyses is presented in Sect. 3. Section 4 discusses the average biases, the stability evaluation of ozone measurements using relative drifts, the temporal evolution of the combination of older and newer satellite data sets and the drifts derived from the combined data. The final section concludes with the findings
5   from the study.

2   Datasets

2.1   LIDAR

The lidar is an active remote sensing instrument based on the interaction between laser radiation and the atmosphere. According to the atmospheric parameter to be
10   measured, lidar systems use various light-matter interactions, such as Rayleigh, Mie and Raman scattering, absorption or fluorescence. The lidar stations considered in our study use the Differential Absorption lidar (DIAL) technique for measuring stratospheric ozone. It provides range-resolved and self-calibrated measurements with high vertical resolution (Schotland, 1974). The technique requires the simultaneous emission of two
15   laser radiations at wavelengths characterised by a different ozone absorption cross-section. For all stations, the ozone-absorbed wavelength used is 308 nm, emitted from a Xenon Chloride excimer laser. The reference wavelength varies at each station between 353 and 355 nm based on its generating method. A Raman cell filled with hydrogen is used for obtaining 353 nm, while the third harmonic of a Nd : YAG laser provides
20   light at 355 nm. The ozone number density is computed from the difference in the slope of the logarithm of the range corrected returned signals. Measurements are performed during night-time under clear sky conditions. In the presence of strong aerosol loading, additional backscattering contaminates the Rayleigh signals. In such conditions, measurements use lidar signals originating from the vibrational Raman scattering of the
25   laser radiation by atmospheric Nitrogen (McGee et al., 1993). The vibrational Raman signals are backscattered at the wavelengths 332 and 385/387 nm corresponding to the Rayleigh wavelengths 308 and 353/355 nm, respectively.

Stability of ozone measurement systems

P. J. Nair et al.

|◄ | ►|

◄ | ►

Back | Close

Full Screen / Esc

Printer-friendly Version

Interactive Discussion

Discussion Paper | Discussion Paper | Discussion Paper | Discussion Paper

Ozone DIAL systems have been making routine operations at MOHp, OHP, Tsukuba, TMF, MLO and Lauder since 1987, 1986, 1988, 1988, 1993 and 1994, respectively. These lidar systems and their ozone retrieval methods are similar. The main difference is in the use of reference wavelength. Most lidar stations use 355 nm as the refer-
⁵ ence wavelength except MOHp and Lauder lidar, which use 353 nm over the whole period and, TMF and MLO lidars used this configuration until 2000 and then changed to 355 nm (Leblanc and McDermid, 2000). Other differences among the lidars are in the receiving data acquisition system and the number of channels used to detect the dynamical range of the lidar signals. For that, the Rayleigh signals are split into high and
¹⁰ low energy channels to retrieve ozone profiles in the upper and mid-lower stratosphere. For instance, at OHP, the receiving system had 2 acquisition channels until 1993. It was then modified to accommodate 6 channels (4 at 308, 355 nm; 2 at 332, 387 nm) in 1994 (Godin-Beekmann et al., 2003). Similar 6 channels are used to measure ozone at Tsukuba (Tatarov et al., 2009) and Lauder (Brinksma et al., 2000). However, only
¹⁵ 2 receiving channels (2 at 308, 353 nm) are used at MOHp (Steinbrecht et al., 2009a) and, 8 channels at TMF (4 at 308, 332 nm; 4 at 355, 387 nm) and MLO (3 at 308, 332 nm; 5 at 355, 387 nm). The precision of lidar ozone measurements degrades with height, with values of 1 % up to 30 km, 2–5 % at 40 km and 5–25 % at 50 km.

The altitude range of most ozone lidar measurements is between the tropopause and
²⁰ 45–50 km, except at Tsukuba, where the highest altitude was 40 km in the beginning of the observation period, decreasing to ∼35 km in 2002 and ∼30 km in 2010. Data from the starting year of observations until 2010 for OHP and Tsukuba and 2011 for other stations are considered for the analysis. As in Nair et al. (2011), here also we have used the OHP ozone lidar profiles re-analysed using NCEP temperature and
²⁵ pressure data and using Bass and Paur (BP) ozone cross-sections (Godin-Beekmann and Nair, 2010). Because the ozone cross-section is sensitive to temperature, a trend of 1 K decade^{-1} can induce an ozone trend of about 0.2 % decade^{-1} (Godin-Beekmann et al., 2003). WMO (2011) has reported a temperature trend of 1.5 K decade^{-1} in the middle and upper stratosphere.

2.2 Ozonesondes

Ozonesonde measurements are characterised by a higher vertical resolution (∼0.2 km) compared to other measurements. The main ozonesonde types are Brewer-Mast (BM) (Brewer and Milford, 1960), Electrochemical Concentration Cell (ECC) (Komhyr, 1969)

5 and Japanese ozonesonde (KC). The measurement principle of sondes is that ambient air is pumped into a chamber containing a potassium iodide (KI) solution, where it gets oxidised by ozone and a current is produced. In the Japanese KC sondes, the concentration of potassium bromide (KBr) is higher than that of KI and it plays an auxiliary role for the above reaction. The amount of ozone in the air sample can be

10 derived from the measurement of the electron flow together with the air volume flow rate delivered by the sonde pump.

Generally, correction factors (CFs) are used to screen the sonde profiles (Tiao et al., 1986). It is the ratio of total ozone provided by a nearby column measuring instrument to the sum of total ozone integrated up to the burst level of sonde measurements and

15 a residual total ozone value evaluated above that level (Logan et al., 1999). The profiles having CF 0.8–1.2 for ECC and KC and 0.9–1.2 for BM sondes are considered of good quality (SPARC, 1998) and are selected in this study. ECC sonde measurements have an uncertainty of about ±5–10 % and provide accurate measurements up to ∼32 km (Smit et al., 2007). Ozone soundings performed at MOHp, OHP, Tateno, Hilo and

20 Lauder are considered here.

BM sondes manufactured by the Mast Keystone Corporation, have been used at MOHp since 1967 (Steinbrecht et al., 1998). They employ a bubbler consisting of an electrochemical cell filled with 0.1 % buffered KI solution in which cathode and anode wires are immersed. The uncertainty of BM sondes is better than 5 % in the strato-

25 sphere. The radiosonde type has been changed from VIZ to Vaisala RS80 in 1996. The BM ozonesonde profiles are normalised by total column data. We used the profiles in 1987–2011 for this study.

At OHP, ECC ozonesondes with 1 % buffered KI cathode sensor solution are performing ozone measurements from 1991 onwards. Type 5A sondes manufactured by

Science Pump Corporation (SPC) were flown from 1991 to 1997 and 1Z series sondes by Environmental Science Corporation (ENSCI) afterwards. The sondes were coupled to Vaisala RS80 radiosondes through a TMAX interface until 2007 and then to Modem M2K2DC radiosondes through an OZAMP interface. We follow the approach

5 for analysing the OHP ozonesonde data described in Nair et al. (2011) except that the ozone partial pressure from the ECC Modem sondes (from June 2007 onwards to the present) were now reprocessed from the current and the pump temperature. Ozonesonde profiles in 1991–2010 are utilised for the analysis.

The KC type ozonesondes, manufactured by Meisei Electric Company, are used

10 at Tateno (hereafter termed as Tsukuba ozonesondes) from 1968 to November 2009 and ECC sondes afterwards. The KC68, KC79 and KC96 were used in 1968–1979, 1979–1997 and from mid-1997 to 2009, respectively. They are based on a carbon-iodine ozone sensor, an electrochemical cell containing platinum gauze as cathode and carbon as anode immersed in an aqueous neutral KI/KBr solution (Fujimoto et al.,

15 1996). In 1979, the double-chambered electrochemical cell is modified to a single cell. The KC sondes are normalised to a total column data and are used here for the period 1988–2009.

ECC sondes made by SPC-4A, 5A and 6A and ENSCI 1Z and 2Z models have been used for measuring ozone at Hilo in 1991–2010. These are connected to Vaisala

20 RS-80-15 type radiosondes using the interface boards En-Sci V2C for all 2Z sondes, TMAX for all 5A, 6A and 1Z sondes and an analog data system for 4A sondes. The data acquisition is made using the Strato version (V) 7.2 program. The cathode sensor solution has been switched from 1 % KI buffered to 2 % KI unbuffered in 1998 and is again changed to 1 % KI buffered in 2005. The integrated ozone column is compared

25 to that of Dobson, but normalisation is not performed (McPeters et al., 1999). In our analysis the correction factor is calculated from the ratio of the Dobson ozone column to the sonde ozone column provided in the data files. Hereafter, Hilo ozonesondes are referred to as the ozonesondes at MLO.

At Lauder, ECC ozonesondes with 1 % KI cathode solution concentration have been flown from 1986 to 1996 and using 0.5 % KI from 1996 to the present. SPC-4A, 5A and 6A series of sondes were used in 1986–1989, 1990–1994 and 1995–1996, respectively, followed by ENSCI-1Z. The VIZ radiosonde was used until 1989 and then Vaisala RS80, coupled with a TMAX interface. Here ozonesonde data are not normalised with total column ozone data, but the data from the sondes containing 1 % solution are multiplied by 0.9743 to put them on the BP scale for Dobson column measurements because the BP cross sections affect the Dobson data on which ozonesonde calibrations are based (Bodeker et al., 1998). Corrections are applied to the ozonesonde values above 200 hPa to account for pump efficiency degradation. The integrated ozone profile is compared to the total column of ozone measured by Dobson spectrophotometer at Lauder and the uncertainty is typically less than 5 %. Ozonesonde measurements from 1986 to 2009 are analysed here.

2.3 Space-based observations

The SBUV(/2) instruments include the original SBUV launched on the NASA (National Aeronautics and Space Administration) NIMBUS-7 satellite in 1978 and the SBUV/2 instruments deployed on the NOAA (National Oceanic and Atmospheric Administration) – 9, 11, 14, 16, 17, 18 and 19 series of satellites from 1984 onwards. The nadir measurement technique is employed to measure ozone profiles from the backscattered UV radiation (250–340 nm). The latitudinal coverage of the measurements is 80° S–80° N and the vertical range is 18–51 km (Bhartia et al., 1996). The long-term measurement uncertainty is $\sim$3 % (DeLand et al., 2004). The vertical resolution of V8 data is 6–8 km and the horizontal resolution is 200 km (Bhartia et al., 2004). We use V8 ozone column measurements from NIMBUS-7, NOAA-9, 11, 16 and 17 in 1985–2007 for this study (Flynn et al., 2009).

SAGE II on Earth Radiation Budget Satellite (ERBS), provided long-term ozone observations from October 1984 to August 2005. The ozone profiles are derived using the solar occultation technique by measuring limb transmittances in seven channels

between 385 and 1020 nm and are inverted using the onion-peeling approach. It measured about 800 profiles per month, with less sampling in summer months at tropical and mid-latitudes. The spatial coverage ranges from 80° S to 80° N from month to month. The vertical range of the ozone profiles is 10–50 km with a vertical resolution of ~1 km and a horizontal resolution of 200 km. The ozone measurements have an uncertainty of ~5 % at 20–45 km and 5–10 % at 15–20 km. The ozone number density profiles retrieved as a function of geometric altitudes processed by the V6.2 algorithm (Wang et al., 2006) for the period 1984–2005 are used.

HALOE on UARS was put into orbit in September 1991, and operated for 15 yr, until 2005. It also measured limb transmittances from the 9.6 μm ozone band utilising the solar occultation technique, and the onion-peeling procedure for the inversion. The latitudinal coverage of the measurements is 80° S–80° N over the course of one year. The vertical range of the ozone profiles is 15–60 km with a vertical resolution of ~2.5 km and a horizontal resolution of 500 km (Russell et al., 1993). Uncertainty of the ozone measurements is about 10 % at 30–64 km and ~30 % at 15 km (Brühl et al., 1996). The ozone volume mixing ratio (VMR) profiles V19 for 1991–2005 are used here.

MLS was launched on UARS in 1991 and its successor aboard Aura in 2004. Both instruments measure thermal emissions from rotational lines of the measured species through the limb of the atmosphere. The 57° inclination of the UARS orbit allowed MLS to observe from 34° on one side of the equator to 80° on the other. The profiles retrieved from 205 GHz have a vertical range of 15–60 km with a resolution of ~3–4 km, and a horizontal resolution of 300 km. The estimated uncertainty of a single profile is 6 % at 21–60 km and 15 % at 16–20 km (Livesey et al., 2003). Aura MLS has better spatial coverage (vertically and horizontally) than UARS MLS, as well as improved resolution. The latitudinal coverage of the measurements is 82° S–82° N. Ozone measurements retrieved from 240 GHz have a vertical range of about 10–73 km and a vertical resolution of 2.5–3 km in the stratosphere. The along-track resolution is ~300–450 km and the estimated uncertainty is about 5–10 % at 13–60 km. Data characterisation and validation of Aura MLS V2.2 data can be found in the work by

Froidevaux et al. (2008); Jiang et al. (2007); Livesey et al. (2008). The ozone VMRs from UARS MLS V5 in 1991–1999 and Aura MLS V3.3 in 2004–2011, screened as suggested in the V3.3 validation report, are used here.

2.4 Stability issues of long-term data sets

Long-term stability is one of the key issues we are interested in this paper. All instruments have different characteristics in this respect. For the ozonesondes, changes in sonde types, manufacturing and sonde preparation are unavoidable in practice, and may affect the long-term stability on the time scale of years to decades. The long-term stability of SBUV(/2) data critically depends on maintaining accurate spectral calibrations over the life-time of one or more instruments. Solar occultation instruments like SAGE II and HALOE are less prone to drifts, because in their measurement they directly compare reference data taken outside the atmosphere with data at various slant paths through the atmosphere. However, accurate pointing and accounting for Rayleigh scattering can be crucial, as is the long-term stability of filter wavelengths and bandpasses. Lidars should have very good long-term stability, because their differential absorption measurement is self-calibrating in principle. It is differential in wavelength, determined very accurately by lasers, and differential in range, which is measured extremely accurately by electronic clocks.

3 Data analysis

The average bias and relative drift of different long and short-term data sets are analysed with respect to the ozone lidar measurements in order to evaluate their consistency and stability. The lidar stations, the respective locations and other observations considered for the analysis are listed in Table 1. The satellite data are extracted around the stations using spatial criteria of ±2.5° latitude and ±5° longitude of each station for SBUV(/2), UARS MLS and Aura MLS, and ±5° latitude and ±10° longitude for the solar

Stability of ozone measurement systems

P. J. Nair et al.

Title Page

Abstract | Introduction

Conclusions | References

Tables | Figures

|◄ | ►|

◄ | ►

Back | Close

Full Screen / Esc

Printer-friendly Version

Interactive Discussion

occultation measurements (SAGE II and HALOE) due to their relatively lower sampling. The total number of measurements of all observational techniques at the lidar stations and the number of coincidences obtained by all data sets from different comparisons are displayed in Fig. 1. The top panel shows the total number of ozone profiles mea-
5 sured by each observation technique above the stations. Regarding the ground-based measurements, about 2000 lidar profiles are available at MOHp, OHP, TMF and MLO for the analysis. Tsukuba and Lauder lidar measured nearly 600 and 1000 profiles, respectively. The number of sonde measurements are larger at MOHp (∼3000) compared to those of OHP (870), Tsukuba (1100), MLO (860) and Lauder (1500) during
10 the analysis period.

Among the satellites, SBUV(/2) and Aura MLS provide the maximum number of measurements (∼8000) during their analysis period of 23 and 8 yr, respectively. They measure nearly the same number of profiles at all regions irrespective of latitude. On the other hand, UARS MLS, SAGE II and HALOE show a clear latitudinal dependence with
15 fewer observations by SAGE II and HALOE at all stations. The solar occultation measurements (SAGE II and HALOE) take more observations above 40° latitude on both hemispheres (e.g. MOHp, OHP and Lauder) and less measurements at other stations. On the contrary, UARS MLS yields more profiles at stations situated below 37° latitude (e.g. Tsukuba, TMF and MLO) and fewer profiles at other stations. Generally, UARS
20 MLS provides more measurements between 34° S to 34° N because of the UARS yaw manoeuvres as stated in Sect. 2.3. Normally, satellite measurements yield more than 1 measurement a day. So in order to be coherent with the ground-based measurements, only one observation per day is considered and is illustrated in panel (b) of Fig. 1.

The analysis is performed using the coincident ozone profiles of various data sets.
25 Coincidences are determined using spatial grids similar to those applied for the data extraction mentioned previously, with a time difference maximum of ±12 h. In order to get a clear idea about the bias and drift of various time series, four different types of comparisons are performed at each station. First various data sets are compared to the lidar measurements and then the same data sets including the lidar ones are

compared to each long-term satellite record (e.g. SBUV(/2), SAGE II and HALOE). Figure 1c shows the total number of coincidences of all measurement techniques with respect to the ozone lidar. Among the lidars, the Tsukuba lidar provides the fewest coincidences due to its comparatively lower measurement frequency. Compared to the stations above 40° N/S, Lauder lidar provides fewer collocations since it has started operation in 1994, about 8 yr after the MOHp and OHP lidars. Figure 1d, e, and f display the number of collocated profiles of the long-term measurements with respect to SBUV(/2), SAGE II and HALOE, respectively. As expected SBUV(/2) and HALOE provide the highest and the lowest number of collocated profiles, respectively, with respect to all other measurement techniques.

3.1 Relative differences and mean biases

In order to quantify the bias of various data records with respect to lidar, the difference time series is computed. As the observing period of lidars is different for various stations, the period of comparisons also differs. The comparison periods of ozonesondes depend on the availability of both lidar and sonde data at the station. In the case of comparison with lidar, the difference between collocated measurements is computed as

$$\Delta O_{3L}(i,j) = \frac{\text{Meas}(i,j) - \text{lidar}(i,j)}{\text{lidar}(i,j)} \times 100\% \tag{1}$$

where i = coincident day, and j = altitude or pressure. "Meas" denotes SBUV(/2), SAGE II, HALOE, UARS MLS, Aura MLS and ozonesondes.

The mean bias of each measurement technique is then calculated by averaging the relative differences over the respective coincident periods with each lidar.

$$\overline{\Delta O_{3L}(j)} = \frac{\sum_{i,j} \Delta O_{3L}(i,j)}{N(j)} \tag{2}$$

where $\overline{\Delta O_{3L}(j)}$ is the average ozone difference and $N(j)$ is the number of collocated profiles at altitude j.

The standard error of the bias is determined as

$$\sigma_N(j) = \frac{\sigma(j)}{\sqrt{N(j)}} \qquad (3)$$

where $\sigma(j)$ is the standard deviation of the relative differences at altitude j.

The estimation of drifts of satellite data requires an evaluation of the stability of the reference measurements, the lidars, in this study. The stability of lidar data is analysed by comparing lidar ozone with SBUV(/2), SAGE II and HALOE as references and by estimating the relative drifts. To compare the drift of lidar measurements with those of other long-term data, SBUV(/2), SAGE II and HALOE ozone data are compared with each other (taking each of them as the reference) in a similar way. For instance, the comparison with SBUV(/2) as the reference is performed as

$$\Delta O_{3B}(i,j) = \frac{\text{Meas}(i,j) - \text{SBUV}(/2)(i,j)}{\text{SBUV}(/2)(i,j)} \times 100\% \qquad (4)$$

with "Meas" as lidar, SAGE II and HALOE. The same procedure is repeated for the comparisons with respect to SAGE II and HALOE, i.e.,

$$\Delta O_{3S}(i,j) = \frac{\text{Meas}(i,j) - \text{SAGE II}(i,j)}{\text{SAGE II}(i,j)} \times 100\% \qquad (5)$$

where "Meas" is lidar, SBUV(/2) and HALOE and

$$\Delta O_{3H}(i,j) = \frac{\text{Meas}(i,j) - \text{HALOE}(i,j)}{\text{HALOE}(i,j)} \times 100\% \qquad (6)$$

where "Meas" is lidar, SBUV(/2) and SAGE II.

3.2   Slopes and standard deviation

The drift between the measurements is computed from the estimation of the slope of the monthly averaged difference time series, using a simple linear regression. The standard deviation (σ_s) of the slope is computed using the same equation as used in Nair et al. (2011), taken from Press et al. (1989).

The derived drift is considered significant if the slope is greater than twice the standard deviation of the slope. Generally, a longer time series with continuous and sufficient number of profiles is needed to determine accurate drifts and to reduce standard deviation to a large extent. The presence of outliers will also result in incorrect drifts. Hence, the analysis excludes the outliers such that the profile consisting of very low and high ozone values at all altitudes are removed from the analysis. In addition, for SAGE II and HALOE, the relative differences exceed 200 % at some altitudes below 17 km and at 45 km. Those altitudes are also removed from the analysis. However, they are very few in number, less than 5 in total for a station.

3.3   Data conversion

The comparison is performed by converting all data to ozone number density as a function of geometric altitude, except for SBUV(/2). Lidar and SAGE II data are given in these units and ozone partial pressures from sondes and VMRs from HALOE and MLS are converted to number density using the pressure–temperature (P/T) data provided in the respective data files. The sondes use the PTU (pressure-temperature-humidity) data measured using the radiosondes coupled to the ozonesondes. SAGE II and HALOE profiles provide the interpolated NCEP P/T data whereas MLS retrieves P/T independently. In order to account for the vertical resolution of MLS ozone, these are compared by integrating the higher resolution lidar profiles within a ±1.5 km altitude band with respect to each MLS altitude level, respectively and then both lidar and MLS data are interpolated to the mean MLS altitude calculated for the comparison period, until 30 km. Above 30 km both lidar and MLS have similar vertical resolution and thus

the comparison is done by interpolating lidar data to MLS altitudes. Comparison between SAGE II and HALOE is also done in the same way, using number density profiles on geometric altitudes by converting HALOE ozone VMRs to number density.

SBUV(/2) provides ozone information as both VMRs and partial columns in Dobson Unit (DU) in which partial ozone columns are used here. Contrary to other comparisons, the partial ozone columns of SBUV(/2) on pressure levels are retained and ozone data from the compared instrument are converted to ozone column in DU. The resulting ozone values are then added above the respective pressure levels and are interpolated logarithmically to the SBUV(/2) pressure levels. Then, ozone in the adjacent layers is subtracted to determine the partial ozone column in each SBUV(/2) layer, which are used for finding the relative differences. As altitude–pressure conversion always induces some bias between the measurements, a special care is needed for its use.

In a previous work (Nair et al., 2011), we have used NCEP data for converting ozone lidar number densities to ozone partial columns for comparing with SBUV(/2). It showed a slightly large drift in the comparison between SBUV(/2) and lidar above 30 km. In a similar study McLinden et al. (2009) also referred to an anomalous temperature trend above 30–35 km for the comparison between SBUV(/2) and SAGE II. Therefore, in this study we took temperature and pressure data from Arletty (Hauchecorne, 1998), an atmospheric model that makes use of the ECMWF (European Centre for Medium Range Weather Forecasts) meteorological analysis until 30 km and MSIS 90 climate model above 30 km for deriving atmosphere profiles, to convert ozone number density from lidars and SAGE II or VMR from HALOE to partial column for the comparison with SBUV(/2). Even if the comparisons are performed on pressure levels, the results are presented on geometric altitudes for the comparison with other measurement techniques too. For that, the approximate altitudes corresponding to the SBUV(/2) mid-pressure levels are calculated using the Arletty data.

The comparison between various lidars and the nearby ozonesondes is performed using the normalised sonde profiles (ozone profiles multiplied by the CF). It should be

P. J. Nair et al.

Title Page

Abstract | Introduction

Conclusions | References

Tables | Figures

◀ | ▶

◀ | ▶

Back | Close

Full Screen / Esc

Printer-friendly Version

Interactive Discussion

noted that the BM sondes at MOHp and KC sondes at Tsukuba are already provided after normalisation, whereas ECC sondes at OHP and MLO are not normalised. So in our analysis, we have multiplied the CF to the OHP and MLO sondes for finding the relative difference and drift.

In short, though we follow similar comparison statistics of Nair et al. (2011), there are some major changes in this study. While Nair et al. (2011) have performed only one type of comparison, with respect to lidar observations, this study uses four different types of comparison statistics to find the drift in the measurements and thus the instrument stability. The average drift is computed to present the global picture of the estimated instrumental drifts. Further, the Aura MLS data are compared to lidar in a different way to compensate with the lower vertical resolution of lidar above 30 km. Also, Arletty P/T data are used instead of NCEP data for the unit conversions. Therefore, there are significant improvements in the analysis presented in this study to find the relative difference, bias and drift.

4   Results and discussion

4.1   Average biases: comparison with lidar measurements

Figure 2 displays the vertical distribution of average relative differences between coincidences of different observations and lidar measurements for various stations. The consistency of ozone measurements can easily be judged from these mean differences. Different measurements show generally a very small bias in comparison to the lidar data, within ±3 % in 20–40 km, except UARS MLS at OHP and Lauder. A very consistent behaviour in the relative differences is shown by all observations at TMF above 21 km except SBUV(/2) between 30 and 40 km. At MLO also all observations display a similar bias. The root mean square (RMS) of mean biases in the 20–40 km altitude range is calculated for all measurements to see which instrument behaves well with the lidar. It is found that among the satellite measurements, HALOE yields the

lowest (2.41 %) and UARS MLS the highest (3.63 %) RMS values at all stations. The average of the RMS values of all observations at each station shows the smallest value (2.45 %) at OHP and the largest value (3.65 %) at Tsukuba.

Generally, the differences are larger in the upper stratosphere (above 40 km) com-
5   pared to those in the middle stratosphere (20–40 km), but are less than those observed in the lower stratosphere (below 20 km). Yet they do not exceed ±7 % in most cases. These large biases above 40 km are likely due to the relatively lower precision of the ozone lidar above 40 km. However, smaller biases are observed with respect to TMF lidar measurements, which implies that these are less noisy in the upper stratosphere.
10 Comparatively larger differences observed below 18 km are mostly due to the large ozone variability in the lower stratosphere. It is noted that the tropopause varies from ∼10 to ∼15 km depending on the season at MOHp, OHP and Lauder, and from ∼12 km in winter to ∼18 km in summer at Tsukuba and TMF, whereas it is located between 16 and 20 km at MLO. Because of the elevated tropopause in all seasons, the analysis
15 excludes the measurements below 21 km at MLO. Near the tropopause the ozone vari-ability is largest, which can be the reason for the observed large differences for all mea-surements below 18 km at Tsukuba and TMF. Besides, as in our analysis, Jiang et al. (2007) also showed some high bias for Aura MLS with the OHP, TMF and MLO lidars in the lower stratosphere, which could be due to the UT/LS (upper troposphere/lower
20 stratosphere) oscillations. In addition, it is a more difficult region to retrieve for satellite measurements.

Large deviations are found at Tsukuba particularly in 15–17 and 40–42 km, as seen in Tatarov et al. (2009). These are possibly due to the fewer coincidences with Tsukuba ozone lidar measurements. The large positive deviations found for UARS MLS below
25 20 km at all stations can be due to the poorer retrieval of UARS MLS. This positive bias near to 100 hPa was also found in the comparison between SAGE II and UARS MLS in all latitudes (Livesey et al., 2003). Aura MLS shows very small deviations above 20 km even though a slight negative bias of ∼5 % is found at OHP and MLO above 38 km. At MLO, it is mainly generated from the MLS temperature data used for the conversion of

MLS ozone VMR to number density. This negative difference above 38 km (3–1.46 hPa) was already shown in Jiang et al. (2007) when compared to lidar and in Boyd et al. (2007) for the comparison with microwave radiometer (MWR) at MLO. Similarly, the differences of SAGE II and Aura MLS with the MWR show positive deviations in the upper stratosphere at Lauder (Boyd et al., 2007), which is same as obtained in our comparison for SAGE II and Aura MLS with the Lauder lidar. Lower negative deviations of Aura MLS at OHP above 40 km, in contrast to the higher bias shown in Nair et al. (2011) implies that differences in vertical resolution can play a significant role in the determination of ozone biases between different instruments.

4.1.1 Application of correction factor

As mentioned in Sect. 2.2, CF is used to screen the sonde profiles in our analysis also and is done at MOHp, OHP, Tsukuba and MLO. So we investigate the differences in the estimated biases in terms of CF. Therefore, the normalised BM and KC sonde profiles are divided by the CF to remove the scaling. Figure 3 shows the average biases obtained for the comparison between lidar and non-normalised (left panel) and normalised (right panel) sondes. The non-normalised BM (at MOHp), KC (at Tsukuba) and ECC (at OHP) sondes provide larger bias compared to the normalised sondes. However, the non-normalised ECC sondes at MLO yield smaller bias than that of the normalised sondes. The non-normalised sondes consistently underestimate ozone at all altitudes at MOHp and OHP. Nevertheless, the non-normalised KC sondes at Tsukuba overestimate ozone above 22 km and underestimate below 19 km, whereas the normalised KC sondes show comparatively larger negative bias below 22 km. In general, multiplication of the CF reduces the bias except at MLO. Besides, the differences between these comparisons, in terms of CF, are not as large for ECC sondes as compared to the BM and KC sondes. In addition, the ozonesondes at MOHp show slightly large bias above 29 km in both cases, which is largely due to the inadequate correction of decreasing pump efficiency in the low pressure regions (Steinbrecht et al., 1998, 2009a).

4.2 Relative drifts

Monthly mean difference time series of the compared data sets are used to evaluate drifts in the ozone measurements because they are less noisy compared to the daily variations and hence, the influence of outliers can be reduced from the drift estimation.
Also, there are possibilities of non-linear drifts for the satellite measurements due to the degradation, particularly for SBUV(/2). But in our analysis, for the consistency, a simple linear regression is applied to these time series and drift is derived from the slope value of the regression.

4.2.1 Comparison with ozone lidar as reference

Lidars are used as a reference for Fig. 4, where drifts are estimated for the data set samples from SBUV(/2), SAGE II, HALOE, Aura MLS and ozonesondes. UARS MLS is excluded from the drift estimation since it is not considered as good for trend studies because of the change of instrument set-up in 1997 due to the failure of one radiometer for the independent P/T retrievals. Generally, the relative drifts are less than $\pm0.3\%\,\mathrm{yr}^{-1}$ at 20–40 km and most of them are insignificant too. However, some significant drifts are observed at some altitudes for SAGE II at OHP and MLO, for HALOE at OHP, TMF and MLO and for SBUV(/2) at TMF and MLO. As we have seen for the biases, drifts are larger below 20 and above 40 km. Among the long-term measurements, SBUV(/2) and ozonesondes provide the smallest drift with respect to all lidars. Aura MLS also exhibits comparable drifts as that of SAGE II and HALOE even if it has only 8 yr of measurements and are significant at some altitudes at MOHp, TMF and MLO. The RMS of the drifts calculated in the 20–40 km altitude range shows the smallest value ($0.27\%\,\mathrm{yr}^{-1}$) for SBUV(/2) and the largest ($1.36\%\,\mathrm{yr}^{-1}$) for Aura MLS. The station average of the RMS values of all measurement techniques provide the lowest value ($0.29\%\,\mathrm{yr}^{-1}$) at OHP and the highest ($2.27\%\,\mathrm{yr}^{-1}$) at Tsukuba.

Aura MLS shows relatively larger negative drifts at MOHp and TMF above 30 km. In order to understand these negative drifts, we analysed the deseasonalised raw ozone

time series (i.e., by considering all observations irrespective of the coincident profiles) from various observations including Aura MLS and lidar, at MOHp and TMF. From the deseasonalised ozone time series, it is observed that MOHp lidar ozone increases from 2007 onwards above 30 km and TMF lidar shows high ozone values in 2008 and 2009 above 30 km compared to all other measurements, which results in significant negative drifts.

Note that the drift in the measurement differences may not entirely be due to the measurement uncertainties of the comparison data sets, as the reference data can also contribute to it. Therefore, accurate diagnosis of the stability of the reference data is a prerequisite in drift studies and hence, the stability of lidar time series is evaluated in the following section.

4.2.2 Comparison of lidar with SBUV(/2), SAGE II and HALOE as references

The stability of ozone lidar measurements at various stations is checked by finding their drifts in comparison with other long-term data sets such as SBUV(/2), SAGE II and HALOE. The derived drifts of all lidars considering SBUV(/2), SAGE II and HALOE as references are shown in Fig. 5a, b and c, respectively. They are almost similar to those in Fig. 4. Generally, all lidars exhibit very small drifts (within $\pm 0.2\,\%\,\text{yr}^{-1}$) with SBUV(/2), but some of these are significant at certain altitudes at MOHp, Tsukuba, TMF and MLO. The drifts with respect to SAGE II and HALOE are slightly larger, but most of them are not significant except the ones at 20–22, 25, 38 and 39 km with SAGE II at MLO. The RMS of the drifts of lidar in the 20–40 km altitude region, averaged over the stations excluding Tsukuba is about 0.16, 0.34 and $0.42\,\%\,\text{yr}^{-1}$ with respect to SBUV(/2), SAGE II and HALOE, respectively. It implies that the lidars can be taken as a reliable reference for drift evaluation of satellite and other ground-based measurements. To corroborate these results, the drifts of other long-term measurements SBUV(/2), SAGE II and HALOE are estimated in a similar manner and are described in the following section.

4.2.3 Comparison of SBUV(/2), SAGE II and HALOE

As mentioned earlier, the relative drifts of SBUV(/2), SAGE II and HALOE are evaluated by comparing them to each other. Figure 6a shows the relative drifts of HALOE at various stations with SAGE II as reference. This comparison shows drifts maximum of about $\pm 0.2\,\%\,\text{yr}^{-1}$ at MOHp and Lauder and $\pm 0.4\,\%\,\text{yr}^{-1}$ at OHP and Tsukuba. At TMF, it is more or less scattered and is less than $\pm 0.5\,\%\,\text{yr}^{-1}$ except at 21–22 and 29–34 km. At MLO also the drifts are more scattered and slightly larger. At MLO, the coincidences are available in 1999–2003 only. This is the reason for the estimated large drifts at MLO. The HALOE–SAGE II drifts are compatible with the no-drift hypothesis, but the uncertainty is too large to detect small drifts. At MLO, the coincidences are available in 1999–2003 only. This is the reason for the estimated large drifts at MLO.

Figure 6b,c represents the relative drifts of SBUV(/2) with SAGE II and HALOE as references, respectively. The relative drifts of SBUV(/2) from both comparisons are very small and most of them are close to zero irrespective of the stations. SBUV(/2)–SAGE II comparison yields smaller drifts than those between SBUV(/2) and HALOE. The former comparison yields around $\pm 0.1\,\%\,\text{yr}^{-1}$ in 20–44 km while the latter leads to about $\pm 0.2\,\%\,\text{yr}^{-1}$ at 21–25, 30–42 km and $\sim 0.5\,\%\,\text{yr}^{-1}$ at 45 km at all stations. The importance is that even if the drifts are very small, some of these are significant particularly in the upper and middle stratosphere. These results are very similar to those mentioned in Nazaryan et al. (2005) and Nazaryan et al. (2007), who compared SBUV/2 (NOAA-11,16) with SAGE II and HALOE, respectively in the latitude bands 50–40° S, 10–20° N, 30–40° N and 40–50° N. In the same manner, Cunnold et al. (2000) calculated drifts between SBUV and SAGE and found very small drifts of $\pm 0.5\,\%\,\text{yr}^{-1}$ in the tropical and mid-latitude regions.

From Figs. 5 and 6, it is obvious that the comparison between SBUV(/2) and all other long-term measurements provides near-zero drifts (or no drifts) at all stations and at all altitudes. Here, the comparison is performed using partial ozone columns on SBUV(/2) pressure levels, which reduces the ozone variability. Moreover, the

coincidences between SBUV(/2) and other measurements provide a continuous time series (or the coincidences are available in all months considered over the time period). These reasons contribute to the smaller drifts.

From all the comparisons, it is clear that only the comparison between SAGE II and
5 HALOE shows relatively larger, but insignificant drifts (Fig. 6a). However, even if the comparison between SAGE II and HALOE produces larger drifts with each other, their comparison with SBUV(/2) and lidar yields very small or near zero drifts. It means that the comparison of similar techniques having a low measurement frequency does not provide an accurate drift estimation from the difference time series. Therefore, the
10 large drift obtained for the comparison between SAGE II and HALOE does not imply that these measurements are unstable for the long-term study. From these estimations, it is inferred that we cannot reach a conclusion on whether measurements are stable or unstable only by comparing two data sets with relatively fewer coincidences in comparison to the other data sets.

15 ### 4.2.4   Average of the drifts of long-term measurements

In order to summarise or to compare globally the magnitude of the drifts of different measurement techniques obtained from various comparisons, the average drifts are computed for each data set at each station and are presented in Fig. 7. For example, the drift of the lidar shown at each station is the average of its drifts (shown in Fig. 5)
20 obtained from the comparisons with SBUV(/2) (Eq. 4), SAGE II (Eq. 5) and HALOE (Eq. 6) as references. Similarly, the mean drift of SBUV(/2) is the average of the drifts obtained from the comparisons with lidar (Eq. 1), SAGE II (Eq. 5) and HALOE (Eq. 6) as references and similarly for SAGE II and HALOE. In a similar way, the standard deviation corresponding to the mean drift of each measurement technique is computed
25 by averaging the standard deviations of each drift obtained from different comparisons. It is just a way to represent the standard deviation and does not show the significance of the drift.

Generally, as found in the previous comparisons, all data sets show small drifts of around $\pm 0.2\,\%\,\text{yr}^{-1}$ at 18–45 km and the measurements are stable too. SAGE II and HALOE ozone at MLO show slightly large drifts, because of the lack of coincidences in most of the years. Below 18 km, the large ozone variability near the tropopause play a pivotal role in deciding the magnitude of the differences.

4.3 Combined data: SAGE II, HALOE and Aura MLS

4.3.1 Time series

It is obvious (from Fig. 4) that the 8 yr data record of Aura MLS yields comparable drifts as of the long-term measurements at all regions. So Aura MLS is a strong candidate for extending terminated observations such as SAGE II and HALOE. Therefore, in this study we assess the possibility of using Aura MLS as a successor of SAGE II and HALOE for ozone trend studies in the low and mid-latitude regions. The combined data sets are computed from the relative differences between the lidar data and SAGE II or HALOE measurements until August 2004, and Aura MLS observations from September 2004 to the end of the respective coincident periods. Before combining data sets of entirely different observational techniques, a correction of bias with respect to lidar measurements needs to be applied. For this, the average biases over the coincident periods of SAGE II, HALOE and Aura MLS, with respect to lidar data, are removed from the corresponding time series of relative differences at each station. Because of the differences in vertical resolutions of SAGE II, HALOE and Aura MLS, the combined data sets are made available at specific reference altitudes (18, 21, 25, 30, 35 and 40 km). The relative differences at these altitudes are calculated by averaging ozone number density within ± 2 km of the altitudes (e.g. 18 ± 2 km). The drifts are also determined from these combined data and are discussed in Sect. 4.3.2.

Figure 8 shows the bias corrected combined time series at MOHp (left panel), OHP (middle panel) and Tsukuba (right panel). At MOHp and OHP, small differences (± 5–7 %) are observed for SAGE II and HALOE in 19–23, 23–27, 28–32 and 33–37 km.

Aura MLS shows very small deviations of less than ±5 % in these altitudes at both stations. At 16–20 and 38–42 km, differences are relatively larger (±10 %) for SAGE II and HALOE and are less than ±7 % for Aura MLS. Even if the Tsukuba time series is characterised by relatively fewer data and large discontinuities, smaller differences are observed. At MOHp, a decreasing tendency is observed in the relative differences of Aura MLS from 28–32 km onwards because of the increase in ozone lidar measurements after 2007, as discussed in Sect. 4.2.1. In addition, a clear seasonal difference is also seen for the comparison with Aura MLS at 38–42 km showing positive deviation in the winter indicating that the Aura MLS ozone is slightly higher than that of MOHp lidar in that season.

Figure 9 displays the bias corrected combined time series at TMF (left panel), MLO (middle panel) and Lauder (right panel). At MLO, the relative differences are less than ±5 %. In the tropics, the ozone variability is very small compared to that of high latitudes, which explains the smaller differences at MLO. At TMF and Lauder, Aura MLS shows differences of ±5 % at all altitudes except at 16–20 km, and SAGE II and HALOE exhibit about ±10 % deviation except at 16–20 km, where the differences exceed ±20 %. At TMF, Aura MLS exhibits negative deviations in 2008 and 2009 from 28–32 km onwards, which can be due to higher lidar ozone during the period as compared to other measurements, as mentioned in Sect. 4.2.1.

4.3.2 Relative drifts of the combined time series

Figure 10 presents the relative drifts estimated from the combined time series (as shown in Figs. 8 and 9) of SAGE II and Aura MLS (left panel), and HALOE and Aura MLS (right panel) at various stations. The drifts are generally within $±0.2 \% \, yr^{-1}$. However, SAGE II/Aura MLS drift at Lauder shows around $±0.2 \% \, yr^{-1}$ at 21, 25, 30 and 35 km and around $±0.3$ and $±0.48 \% \, yr^{-1}$ at 18 and 40 km, respectively. These large values are due to the fact that the first two measurements in the beginning of the period show slightly larger difference for SAGE II versus lidar as shown in Fig. 9. The removal of those two measurements results in a very small drift of less than $±0.2 \% \, yr^{-1}$ over

the whole range (shown as dashed lines in the left panel of Fig. 10). At Tsukuba, drifts are relatively larger at some altitudes compared to that at other stations. Generally, the combined data show insignificantly small drifts. It indicates that the combination of these satellite observations provides a potential long-term data set for the evaluation of long-term ozone trends in the stratosphere.

5 Conclusions

An extensive analysis of stratospheric ozone measurements at different NDACC lidar stations (MOHp, OHP, Tsukuba, TMF, MLO and Lauder) is performed in this study. The diagnosis is done by comparing various long and short-term satellite observations of SBUV(/2), SAGE II, HALOE, UARS MLS and Aura MLS as well as ozonesonde measurements at the respective stations.

The relative difference (or bias) of all measurement techniques is found by comparing them with respect to lidar measurements in their respective coincident periods. All measurement techniques (satellites and sondes) agree well with all lidars, with average biases of less than $\pm 3\%$, in the 20–40 km range. In order to detect ozone trends on the order of a few $\%\,\mathrm{decade}^{-1}$, stability of long-term measurements is essential. This is particularly important for long-term ground-based and satellite sensors, which may be subject to some degradation during their life time. Therefore, in this study we examine the stability of each measuring system by investigating the magnitude of the drifts. This is attained first by comparing all measurements with respect to lidars, which yields drifts of less than $\pm 0.3\%\,\mathrm{yr}^{-1}$ at 20–40 km for all observations. Aura MLS with 8 yr of observation also shows drifts that are comparable to those from the long-term data sets at all stations. Below 20 and above 40 km relative differences and drifts are larger, mostly due to discontinuity in the time series, smaller ozone values and higher uncertainty of ozone observations in these altitude regions. In addition, in the lower stratosphere larger atmospheric variability at the mid-latitude stations and a higher tropopause at the tropical station also contribute to the observed large biases and drifts.

A successful evaluation of biases and drifts depends on the stability of the reference data and hence the drifts of ozone lidar measurements with respect to the longer data sets SBUV(/2), SAGE II and HALOE are estimated. The relative drifts of lidar are nearly zero at most altitudes. Similarly, the drifts of SBUV(/2), SAGE II and HALOE are estimated by comparing them with each other. Comparison between SAGE II and HALOE shows drifts with maximum of ± 0.2–$0.4\,\%\,yr^{-1}$ in 20–45 km whereas the comparison of SBUV(/2) with lidar, SAGE II and HALOE produces near zero drifts. Because of successive instruments, SBUV(/2) provides daily global measurements over the whole period with a large number of collocated profiles, and thus a very accurate evaluation of drift of the data is performed. So a sufficient number of continuous profiles is an important factor for deducing accurate drifts with meaningful statistics. The averages of the drifts of long-term measurements obtained from various comparisons are within $\pm 0.2\,\%\,yr^{-1}$ in 20–45 km. Therefore, the long-term measurements considered here are stable at the respective latitude bands.

As the various ozone measurement techniques yield consistent results, it is useful to combine different ozone measurements to establish a long-term data set for further analyses and trend studies. Hence, a bias-corrected combined time series is constructed using the relative differences of SAGE II and HALOE, with respect to lidar data, with that of Aura MLS and the relative drifts are estimated. It shows near-zero drifts at most altitudes for all the considered latitude bands. So the combination of the older data sets, SAGE II and HALOE, with Aura MLS is shown to be very suitable for the estimation of long-term ozone trends.

Therefore, this work satisfies one of the main goals of NDACC, the calibration and validation of satellite measurements over several decades at different latitude bands. This study is unique as it establishes for the first time the bias and drift of short and long-term data for a number of ground-based stations using at least four different comparison methods and evaluates drifts of the long and short-term combined data sets. It demonstrates that long-term NDACC lidar ozone time series are suitable for the evaluation of the stability of satellite measurements and the estimation of ozone trends.

Institut national des **sciences** de **l'Univers**

References

Ancellet, G. and Beekmann, M.: Evidence for changes in the ozone concentrations in the free troposphere over Southern France from 1976 to 1995, Atmos. Environ., 31, 2835–2851, 1997.

Bhartia, P. K., McPeters, R. D., Mateer, C. L., Flynn, L. E., and Wellemeyer, C.: Algorithm for the

estimation of vertical ozone profiles from the backscattered ultraviolet technique, J. Geophys. Res., 101, 18793–18806, 1996. 480

Bhartia, P. K., Wellemeyer, C. G., Taylor, S. L., Nath, N., and Gopalan. A.: Solar backscatter ultraviolet (SBUV) version 8 profile algorithm, in: Proceedings of the XX Quadrennial Ozone Symposium, edited by: Zerefos, C. S., Int. Ozone Comm., Athens, Greece, 295–296, 2004. 480

Bodeker, G., Boyd, I., and Matthews, W.: Trends and variability in vertical ozone and temperature profiles measured by ozonesondes at Lauder, New Zealand: 1986–1996, J. Geophys. Res., 103, 28661–28681, 1998. 480

Boyd, I. S., Parrish, A. D., Froidevaux, L., von Clarmann, T., Kyrölä, E., Russell III, J. M., and Zawodny, J. M.: Ground-based microwave ozone radiometer measurements compared with Aura-MLS v2.2 and other instruments at two Network for Detection of Atmospheric Composition Change sites, J. Geophys. Res., 112, D24S33, doi:10.1029/2007JD008720, 2007. 490

Brewer, A. W. and Milford, J., R.: The Oxford-Kew Ozone Sonde, P. R. Soc. Lond. A, 256, 470–495, 1960. 478

Brinksma, E. J., Bergwerff, J. B., Bodeker, G. E., Boersma, K. F., Boyd, I. S., Connor, B. J., deHaan, J. F., Hogervorst, W., Hovenier, J. W., Parrish, A., Tsou, J. J., Zawodny, J. M., and Swart, D. P. J.: Validation of 3 years of ozone measurements over Network for the Detection of Stratospheric Change station Lauder, New Zealand, J. Geophys. Res., 105, 17291–17306, 2000. 477

Brühl, C., Roland Drayson, S., Russell III, J. M., Crutzen, P. J., McInerney, J. M., Purcell, P. N., Claude, H., Gernandt, H., McGee, T. J., McDermid, I. S., and Gunson, M. R.: Halogen Occultation Experiment ozone channel validation, J. Geophys. Res., 101, 10217–10240, 1996. 481

Cunnold, D., Newchurch, M., Flynn, L., Wang, H., Russell, J. M., McPeters, R., Zawodny, J., and Froidevaux, L.: Uncertainties in upper stratospheric ozone trends from 1979 to 1996, J. Geophys. Res., 105, 4427–4444, 2000. 493

DeLand, M. T., Huang, L.-K., Taylor, S. L., McKay, C. A., Cebula, R. P., Bhartia, P. K., and McPeters, R. D.: Long-term SBUV and SBUV/2 instrument calibration for Version 8 ozone data, in: Proceedings of the XX Quadrennial Ozone Symposium, edited by: Zerefos, C., Univ. of Athens, Greece, 321–322, 2004. 480

Dhomse, S., Weber, M., Wohltmann, I., Rex, M., and Burrows, J. P.: On the possible causes

Stability of ozone measurement systems

P. J. Nair et al.

of recent increases in northern hemispheric total ozone from a statistical analysis of satellite data from 1979 to 2003, Atmos. Chem. Phys., 6, 1165–1180, doi:10.5194/acp-6-1165-2006, 2006. 474

Farman, J. C., Gardiner, B. G., and Shanklin, J. D.: Large losses of total ozone in the Antarctica reveal seasonal ClO_x/NO_x interaction, Nature, 315, 207–210, 1985. 473

Flynn, L. E., McNamara, D., Beck, C. T., Petropavlovskikh, I., Beach, E., Pachepsky, Y., Li, Y. P., Deland, M., Huang, L.-K., Long, C. S., Tiruchirapalli, R., and Taylor, S.: Measurements and products from the Solar Backscatter Ultraviolet (SBUV/2) and Ozone Mapping and Profiler Suite (OMPS) instruments, Int. J. Remote Sens., 30, 4259–4272, doi:10.1080/01431160902825040, 2009. 480

Froidevaux, L., Jiang, Y. B., Lambert, A., Livesey, N. J., Read, W. G., Waters, J. W., Browell, E. V., Hair, J. W., Avery, M. A., McGee, T. J., Twigg, L. W., Sumnicht, G. K., Jucks, K. W., Margitan, J. J., Sen, B., Stachnik, R. A., Toon, G. C., Bernath, P. F., Boone, C. D., Walker, K. A., Filipiak, M. J., Harwood, R. S., Fuller, R. A., Manney, G. L., Schwartz, M. J., Daffer, W. H., Drouin, B. J., Cofield, R. E., Cuddy, D. T., Jarnot, R. F., Knosp, B. W., Perun, V. S., Snyder, W. V., Stek, P. C., Thurstans, R. P., and Wagner, P. A.: Validation of Aura Microwave Limb Sounder stratospheric ozone measurements, J. Geophys. Res., 113, D15S20, doi:10.1029/2007JD008771, 2008. 482

Fujimoto, T., Uchino, O., and Nagai, T.: Four year intercomparison of ozone lidar, ozonesonde and SAGE II data, in: Proceedings of the XVIII Quadrennial Ozone Symposium, edited by: Bojkov, R. and Visconti, G., L'Aquila, Italy, 127–130, 1996. 479

Godin-Beekmann, S. and Nair, P. J.: Sensitivity of stratospheric ozone lidar measurements on ozone cross-section, available at: http://igaco-o3.fmi.fi/ACSO, last access: 28 October 2011, 2010. 477

Godin-Beekmann, S., Porteneuve, J., and Garnier, A.: Systematic DIAL lidar monitoring of the stratospheric ozone vertical distribution at Observatoire de Haute-Provence (43.92° N, 5.71° E), J. Environ. Monitor., 5, 57–67, 2003. 477

Harris, N. R. P., Kyrö, E., Staehelin, J., Brunner, D., Andersen, S.-B., Godin-Beekmann, S., Dhomse, S., Hadjinicolaou, P., Hansen, G., Isaksen, I., Jrrar, A., Karpetchko, A., Kivi, R., Knudsen, B., Krizan, P., Lastovicka, J., Maeder, J., Orsolini, Y., Pyle, J. A., Rex, M., Vanicek, K., Weber, M., Wohltmann, I., Zanis, P., and Zerefos, C.: Ozone trends at northern mid- and high latitudes – a European perspective, Ann. Geophys., 26, 1207–1220, doi:10.5194/angeo-26-1207-2008, 2008. 474

Hauchecorne, A., Ether, Service Arletty, Atmospheric Model Description, ETH-ACR-AR-DM-001, 22 p., 1998. 487

Jiang, Y. B., Froidevaux, L., Lambert, A., et al.: Validation of Aura Microwave Limb Sounder Ozone by ozonesonde and lidar measurements, J. Geophys. Res., 112, D24S34, doi:10.1029/2007JD008776, 2007. 482, 489, 490

Jones, A., Urban, J., Murtagh, D. P., Eriksson, P., Brohede, S., Haley, C., Degenstein, D., Bourassa, A., von Savigny, C., Sonkaew, T., Rozanov, A., Bovensmann, H., and Burrows, J.: Evolution of stratospheric ozone and water vapour time series studied with satellite measurements, Atmos. Chem. Phys., 9, 6055–6075, doi:10.5194/acp-9-6055-2009, 2009. 474

Komhyr, W. D.: Electrochemical concentration cells for gas analysis, Ann. Geophys., 25, 203–210, 1969,
http://www.ann-geophys.net/25/203/1969/. 478

Leblanc, T. and McDermid, I.: Stratospheric ozone climatology from lidar measurements at Table Mountain ($34.4°$ N, $117.7°$ W) and Mauna Loa ($19.5°$ N, $155.6°$ W), J. Geophys. Res., 105, 14613–14623, 2000. 477

Livesey, N. J., Read, W. G., Froidevaux, L., Waters, J. W., Santee, M. L., Pumphrey, H. C., Wu, D. L., Shippony, Z., and Jarnot, R. F.: The UARS Microwave Limb Sounder version 5 data set: theory, characterization, and validation, J. Geophys. Res., 108, 4378, doi:10.1029/2002JD002273, 2003. 481, 489

Livesey, N. J., Filipiak, M. J., Froidevaux, L., Read, W. G., Lambert, A., Santee, M. L., Jiang, J. H., Pumphrey, H. C., Waters, J. W., Cofield, R. E., Cuddy, D. T., Daffer, W. H., Drouin, B. J., Fuller, R. A., Jarnot, R. F., Jiang, Y. B., Knosp, B. W., Li, Q. B., Perun, V. S., Schwartz, M. J., Snyder, W. V., Stek, P. C., Thurstans, R. P., Wagner, P. A., Avery, M., Browell, E. V., Cammas, J.-P., Christensen, L. E., Diskin, G. S., Gao, R.-S., Jost, H.-J., Loewenstein, M., Lopez, J. D., Nedelec, P., Osterman, G. B., Sachse, G. W., and Webster, C. R.: Validation of Aura Microwave Limb Sounder O_3 and CO observations in the upper troposphere and lower stratosphere, J. Geophys. Res., 113, D15S02, doi:10.1029/2007JD008805, 2008. 482

Logan, J. A., Megretskaia, I. A., Miller, A. J., Tiao, G. C., Choi, D., Zhang, L., Stolarski, R. S., Labow, G. J., Hollandsworth, S. M., Bodeker, G. E., Claude, H., De Muer, D., Kerr, J. B., Tarasick, D. W., Oltmans, S. J., Johnson, B., Schmidlin, F., Staehelin, J., Viatte, P., and Uchino, O.: Trends in the vertical distribution of ozone: a comparison of two analyses of ozonesonde data, J. Geophys. Res., 104, 26373–26399, 1999. 478

Stability of ozone measurement systems

P. J. Nair et al.

Title Page

Abstract | Introduction

Conclusions | References

Tables | Figures

|◄ | ►|

◄ | ►

Back | Close

Full Screen / Esc

Printer-friendly Version

Interactive Discussion

McGee, T. J., Gross, M., Ferrare, R., Heaps, W., and Singh, U.: Raman dial measurements of stratospheric ozone in the presence of volcanic aerosols, Geophys. Res. Lett., 20, 955–958, 1993. 476

McLinden, C. A., Tegtmeier, S., and Fioletov, V.: Technical Note: A SAGE-corrected SBUV zonal-mean ozone data set, Atmos. Chem. Phys., 9, 7963–7972, doi:10.5194/acp-9-7963-2009, 2009. 487

McPeters, R. D., Hofmann, D. J., Clark, M., Flynn, L., Froidevaux, L., Gross, M., Johnson, B., Koenig, G., Liu, X., McDermid, S., McGee, T., Murcray, F., Newchurch, M. J., Oltmans, S., Parrish, A., Schnell, R., Singh, U., Tsou, J. J., Walsh, T., and Zawodny, J. M.: Results from the 1995 Stratospheric Ozone Profile Intercomparison at Mauna Loa, J. Geophys. Res., 104, 30505–30514, 1999. 479

Nair, P. J., Godin-Beekmann, S., Pazmiño, A., Hauchecorne, A., Ancellet, G., Petropavlovskikh, I., Flynn, L. E., and Froidevaux, L.: Coherence of long-term stratospheric ozone vertical distribution time series used for the study of ozone recovery at a northern mid-latitude station, Atmos. Chem. Phys., 11, 4957–4975, doi:10.5194/acp-11-4957-2011, 2011. 475, 477, 479, 486, 487, 488, 490

Nazaryan, H. and McCormick, M. P.: Comparisons of Stratospheric Aerosol and Gas Experiment (SAGE II) and Solar Backscatter Ultraviolet Instrument (SBUV/2) ozone profiles and trend estimates, J. Geophys. Res., 110, D17302, doi:10.1029/2004JD005483, 2005. 493

Nazaryan, H., McCormick, M. P., and Russell III, J. M.: Comparative analysis of SBUV/2 and HALOE ozone profiles and trends, J. Geophys. Res., 112, D10304, doi:10.1029/2006JD007367, 2007. 493

Newchurch, M. J., Yang, E.-S., Cunnold, D. M., Reinsel, G. C., and Zawodny, J. M.: Evidence for slowdown in stratospheric ozone loss: first stage of ozone recovery, J. Geophys. Res., 108, 4507, doi:10.1029/2003JD003471, 2003. 474

Press, W. H., Flannery, B. P., Teukolsky, S. A., and Vetterling, W. T. (Eds.): Numerical Recipes, Cambridge University Press, Cambridge, UK, 504–508, 1989. 486

Reinsel, G. C., Weatherhead, E. C., Tiao, G. C., Miller, A. J., Nagatani, R. M., Wuebbles, D. J., and Flynn, L. E.: On detection of turnaround and recovery in trend for ozone, J. Geophys. Res., 107, 4078, doi:10.1029/2001JD000500, 2002. 474

Russell, J. M., Gordley, L. L., Park, J. H., Drayson, S. R., Hesketh, W. D., Cicerone, R. J., Tuck, A. F., Frederick, J. E., Harries, J. E., and Crutzen, P. J.: The Halogen Occultation Experiment, J. Geophys. Res., 98, 10777–10797, 1993. 481

Stability of ozone measurement systems

P. J. Nair et al.

Title Page

Abstract | Introduction

Conclusions | References

Tables | Figures

|◄ | ►|

◄ | ►

Back | Close

Full Screen / Esc

Printer-friendly Version

Interactive Discussion

Schotland, R. M.: Errors in the lidar measurement of atmospheric gases by differential absorption, J. Appl. Meteorol., 13, 71–77, 1974. 476

Smit, H. G. J., Straeter, W., Johnson, B. J., Oltmans, S. J., Davies, J., Tarasick, D. W., Hoegger, B., Stubi, R., Schmidlin, F. J., Northam, T., Thompson, A. M., Witte, J. C., Boyd, I., and Posny, F.: Assessment of the performance of ECC ozonesondes under quasi flight conditions in the environmental simulation chamber: insights from the Juelich Ozone Sonde Intercomparison Experiment (JOSIE), J. Geophys. Res., 112, D19306, doi:10.1029/2006JD007308, 2007. 478

Steinbrecht, W., Schwarz, R., and Claude, H.: New pump correction for the Brewer–Mast ozone sonde: determination from experiment and instrument intercomparisons, J. Atmos. Ocean. Tech., 15, 144–156, 1998. 478, 490

Steinbrecht, W., Claude, H., Schönenborn, F., McDermid, I. S., Godin, S., Song, T., Swart, D. P. J., Meijer, Y. J., Bodeker, G. E., Connor, B. J., Kämpfer, N., Hocke, K., Calisesi, Y., Schneider, N., de la Noë, J., Parrish, A. D., Boyd, I. S., Brühl, C., Steil, B., Giorgetta, M. A., Manzini, E., Thomason, L. W., Zawodny, J. M., McCormick, M. P., Russell III, J. M., Bhartia, P. K., Stolarski, R. S., and Hollandsworth-Frith, S. M.: Long-term evolution of upper stratospheric ozone at selected stations of the Network for the Detection of Stratospheric Change (NDSC), J. Geophys. Res., 111, D10308, doi:10.1029/2005JD006454, 2006. 474

Steinbrecht, W., McGee, T. J., Twigg, L. W., Claude, H., Schönenborn, F., Sumnicht, G. K., and Silbert, D.: Intercomparison of stratospheric ozone and temperature profiles during the October 2005 Hohenpeißenberg Ozone Profiling Experiment (HOPE), Atmos. Meas. Tech., 2, 125–145, doi:10.5194/amt-2-125-2009, 2009a. 477, 490

Steinbrecht, W., Claude, H., Schönenborn, F., McDermid, I. S., Leblanc, T., Godin-Beekmann, S., Keckhut, P., Hauchecorne, A., Van Gijsel, J. A. E., Swart, D. P. J., Bodeker, G. E., Parrish, A., Boyd, I. S., Kämpfer, N., Hocke, K., Stolarski, R. S., Frith, S. M., Thomason, L. W., Remsberg, E. E., Von Savigny, C., Rozanov, A., and Burrows, J. P.: Ozone and temperature trends in the upper stratosphere at five stations of the Network for the Detection of Atmospheric Composition Change, Int. J. Remote Sens., 30, 3875–3886, doi:10.1080/01431160902821841, 2009b. 474

SPARC (Stratospheric Processes and Their Role in Climate): Assessment of Trends in the Vertical Distribution of Ozone, Rep. 1, edited by: Harris, N., Hudson, R., and Phillips, C., World Meteorol. Organ., Geneva, 1998. 478

Tatarov, B., Nakane, H., Park, Ch. B., Sugimoto, N., and Matsui, I.: Lidar observation of long-

Stability of ozone measurement systems

P. J. Nair et al.

Title Page

Abstract | Introduction

Conclusions | References

Tables | Figures

◄ | ►

Back | Close

Full Screen / Esc

Printer-friendly Version

Interactive Discussion

term trends and variations of stratospheric ozone and temperature over Tsukuba, Japan, Int. J. Remote Sens., 30, 3951–3960, 2009. 477, 489

Tiao, G. C., Reinsel, G. C., Pedrick, J. H., Allenby, G. M., Mateer, C. L., Miller, A. J. and, DeLuisi, J. J.: A statistical trend analysis of ozonesonde data, J. Geophys. Res., 91, 13121–13136, doi:10.1029/JD091iD12p13121, 1986. 478

Wang, P. H., Cunnold, D. M., Trepte, C. R., Wang, H. J., Jing, P., Fishman, J., Brackett, V. G., Zawodney, J. M., and Bodeker, G. E.: Ozone variability in the midlatitude upper troposphere and lower stratosphere diagnosed from a monthly SAGE II climatology relative to the tropopause, J. Geophys. Res., 111, D21304, doi:10.1029/2005JD006108, 2006. 481

Weatherhead, E. C. and Andersen, S. B.: The search for signs of recovery of the ozone layer, Nature, 441, 39–45, doi:10.1038/nature04746, 2006. 474

WMO (World Meteorological Organization): Scientific assessment of ozone depletion: 2006, Global Ozone Research and Monitoring Project, Rep. 25, Geneva, Switzerland, 2007. 474

WMO (World Meteorological Organization): Scientific assessment of ozone depletion: 2010, Global Ozone Research and Monitoring Project, Rep. 52, Geneva, Switzerland, 2011. 477

Yang, E.-S., Cunnold, D. M., Salawitch, R. J., McCormick, M. P., Russell III, J., Zawodny, J. M., Oltmans, S., and Newchurch, M. J.: Attribution of recovery in lower-stratospheric ozone, J. Geophys. Res., 111, D17309, doi:10.1029/2005JD006371, 2006. 474

Zanis, P., Maillard, E., Staehelin, J., Zerefos, C., Kosmidis, E., Tourpali, K., and Wohltmann, I.: On the turnaround of stratospheric ozone trends deduced from the reevaluated Umkehr record of Arosa, Switzerland, J. Geophys. Res., 111, D22307, doi:10.1029/2005JD006886, 2006. 474

Title Page

Abstract | Introduction

Conclusions | References

Tables | Figures

◀ | ▶

◀ | ▶

Back | Close

Full Screen / Esc

Printer-friendly Version

Interactive Discussion

Table 1. Various NDACC lidar stations, their locations, the period of observations of lidar and the analysis period of ozonesondes used in this study are given. The satellite data sets utilised for the study and their observational periods are also noted.

Station	Location Lat	Lon	Period Lidar	ozonesondes	Instrument	Period
MOHp	47.8° N	11.0° E	1987–2011	1987–2011	SBUV(/2)	1984–2007
OHP	43.9° N	5.7° E	1985–2010	1991–2010	SAGE II	1984–2005
Tsukuba	36.0° N	140.0° E	1988–2010	1988–2009	HALOE	1991–2005
TMF	34.5° N	117.7° W	1988–2011	–	UARS MLS	1991–1999
MLO	19.5° N	155.6° W	1993–2011	1993–2010	Aura MLS	2004–2011
Lauder	45.0° S	169.7° E	1994–2011	1994–2009		

Printer-friendly Version

Interactive Discussion
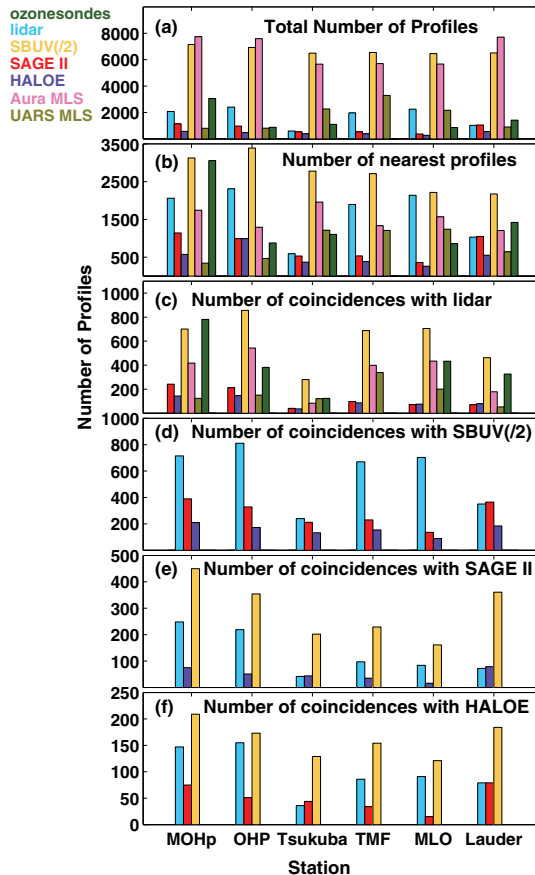
Fig. 1. Total number of profiles of all data sets at various stations **(a)**, the total number of profiles considering one measurement per day **(b)**, the total number of coincidences of different observations with lidar **(c)** and the total number of coincidences of the long-term measurements with SBUV(/2) **(d)**, SAGE II **(e)** and HALOE **(f)**.
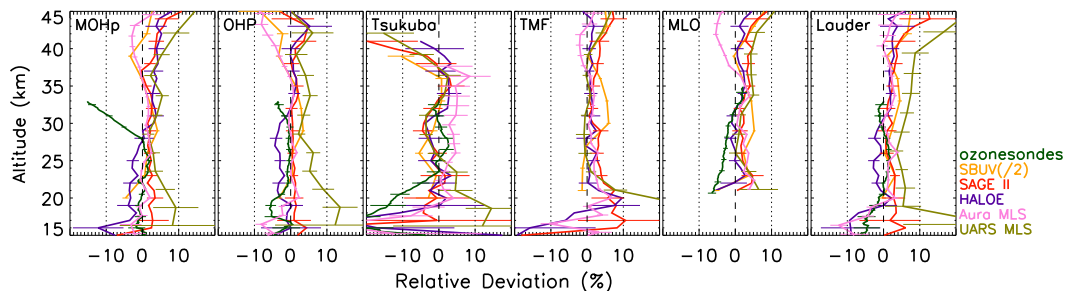
Fig. 2. Vertical distribution of the average relative differences of the coincident ozone profiles of different datasets with various lidar measurements $\left[\frac{1}{N}\Sigma\left(100\times\frac{\text{Meas}-\text{lidar}}{\text{lidar}}\right)\right]$. The dashed and dotted vertical lines represent 0 and ±10 %, respectively and the error bars correspond to twice the standard error.
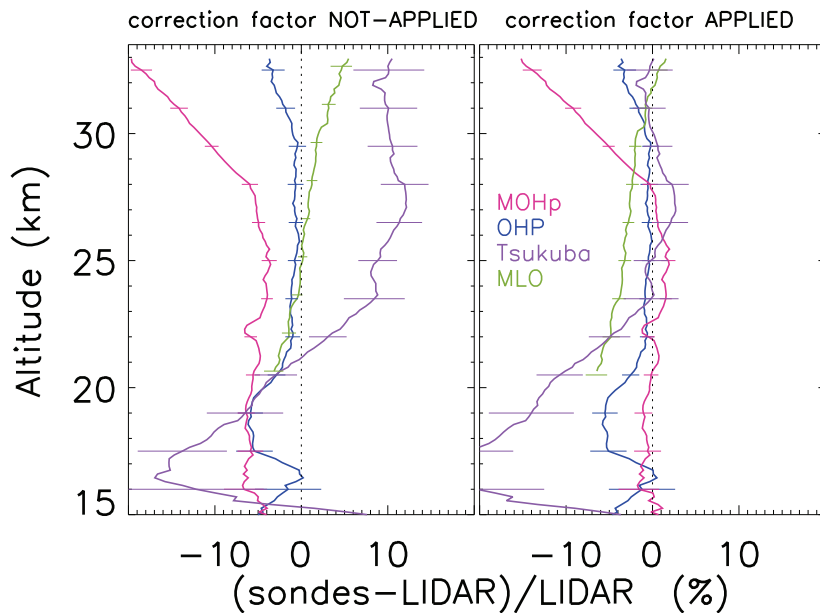
Fig. 3. The average bias of sonde measurements, without (left panel) and with (right panel) multiplying the profiles by the correction factor, obtained for the comparison with lidar at MOHp, OHP, Tsukuba and MLO. The dotted vertical line represents 0 % and the error bars correspond to twice the standard error.

Stability of ozone measurement systems

P. J. Nair et al.

Title Page	
Abstract	Introduction
Conclusions	References
Tables	Figures
◄◄	►►
◄	►
Back	Close
Full Screen / Esc	
Printer-friendly Version	
Interactive Discussion	
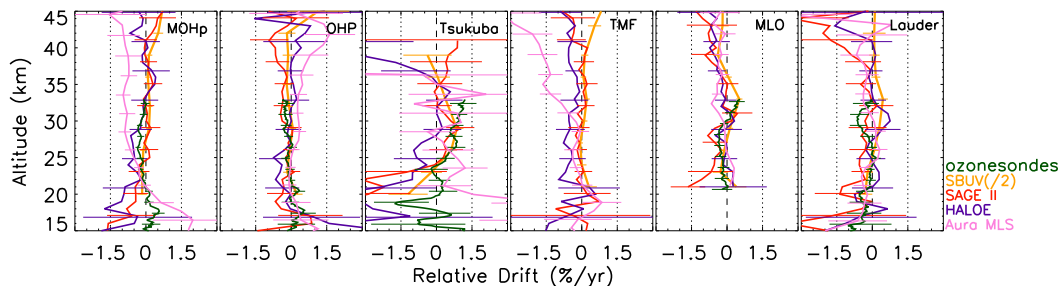
Fig. 4. Vertical distribution of the slopes evaluated from the monthly averaged difference time series of all observations with the lidar measurements at various regions $\left(100 \times \frac{\text{Meas}-\text{lidar}}{\text{lidar}}\right)$. The error bars represent twice the standard deviation of the slope. The dashed vertical line represents $0\,\%\,\text{yr}^{-1}$ and the dotted vertical lines represent $\pm 1.5\,\%\,\text{yr}^{-1}$.
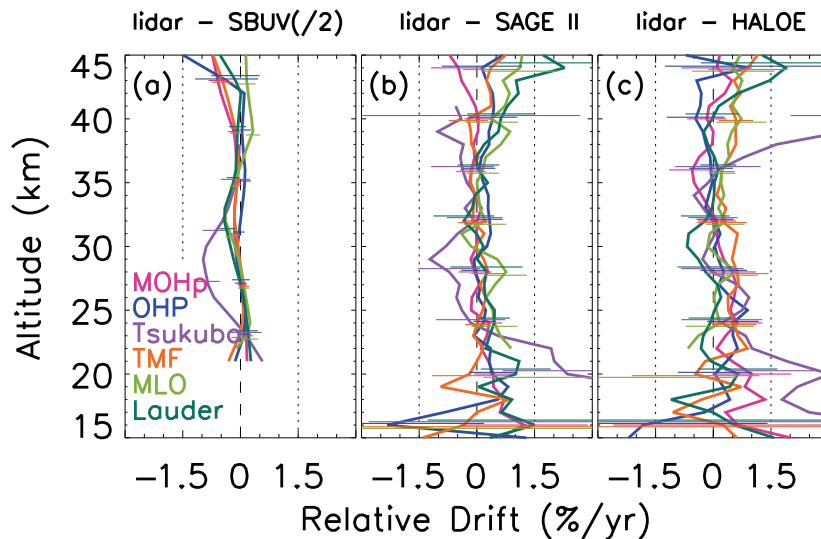
Fig. 5. The drifts of various lidars for the comparison with SBUV(/2), SAGE II and HALOE as references $\left(100 \times \frac{\text{lidar} - \text{ref}}{\text{ref}}\right)$. The error bars correspond the 95 % confidence interval of the slope.
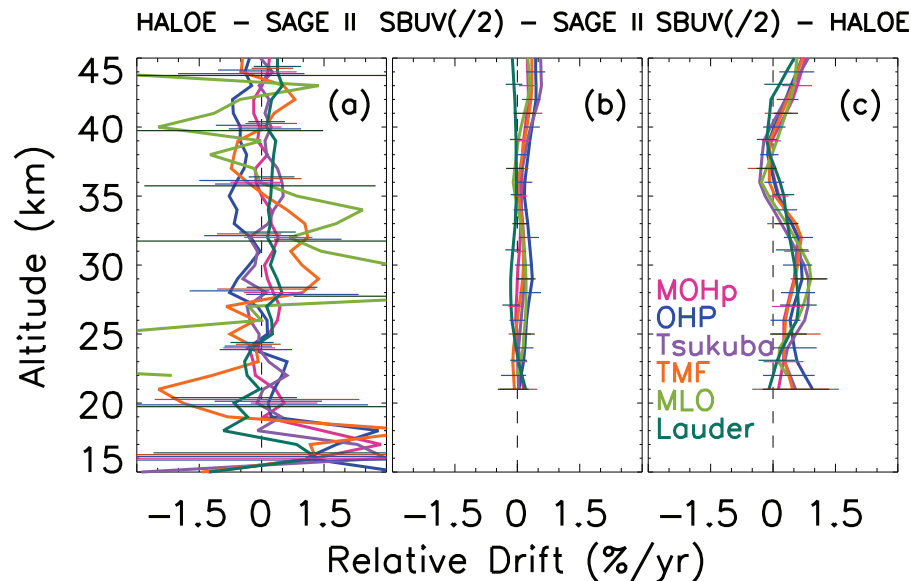
Fig. 6. **(a)** The drifts of HALOE in comparison with SAGE II as reference $\left(100 \times \frac{\text{HALOE}-\text{SAGE II}}{\text{SAGE II}}\right)$ at various stations. **(b)** The drifts of SBUV(/2) with SAGE II as reference $\left(100 \times \frac{\text{SBUV(/2)}-\text{SAGE II}}{\text{SAGE II}}\right)$. **(c)** Same as (b), but with HALOE as reference $\left(100 \times \frac{\text{SBUV(/2)}-\text{HALOE}}{\text{HALOE}}\right)$. The error bars represent twice the standard deviation of the slope.
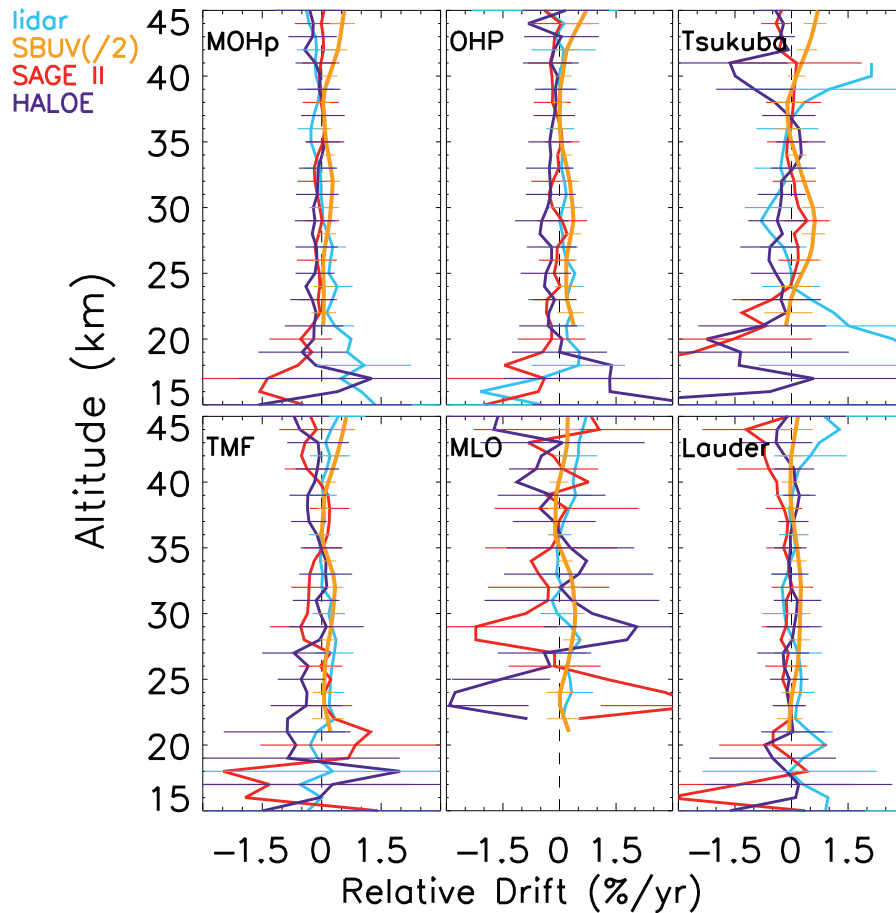
Fig. 7. The mean drifts estimated for the long-term observations with respect to other long-term measurements as references. The error bars represent twice the average of the standard deviations of the slopes obtained from different comparisons.
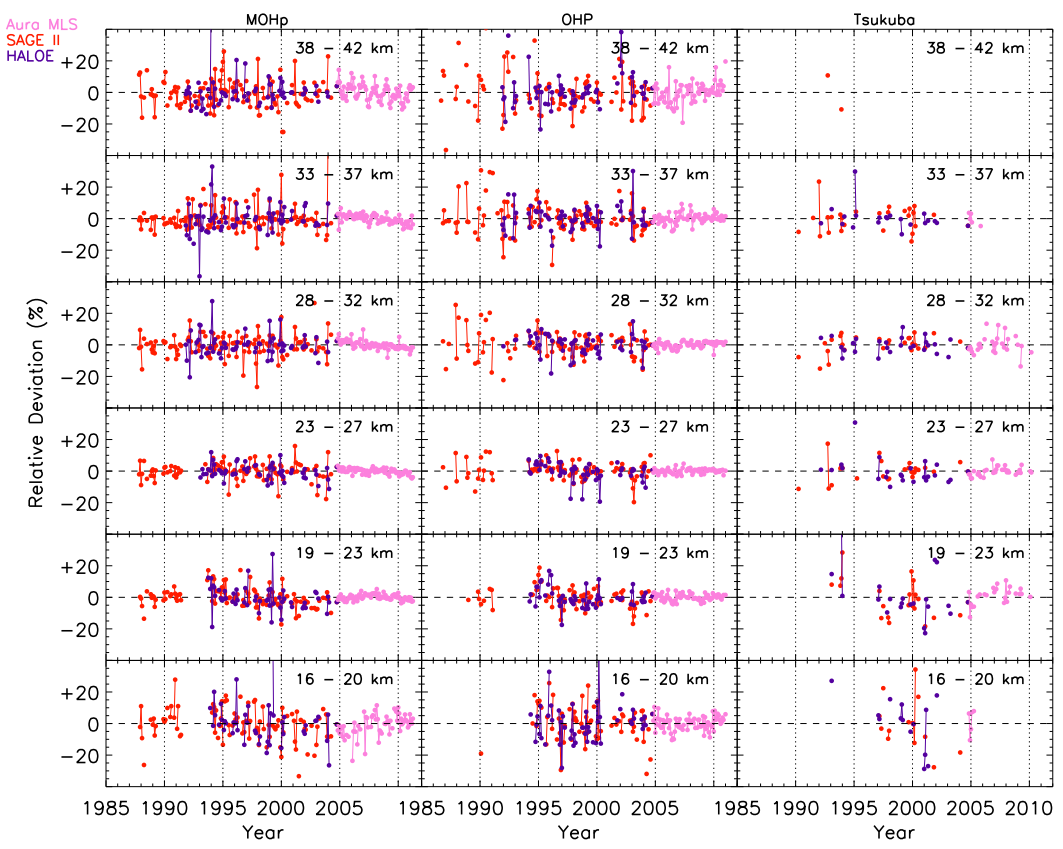
Fig. 8. Temporal evolution of the bias removed monthly averages of the relative differences of SAGE II, HALOE and Aura MLS with ozone lidar at MOHp (left panel) , OHP (middle panel) and Tsukuba (right panel). The dashed horizontal line represents 0 %.

Stability of ozone measurement systems

P. J. Nair et al.

Title Page

Abstract | Introduction

Conclusions | References

Tables | Figures

◀ | ▶

◀ | ▶

Back | Close

Full Screen / Esc

Printer-friendly Version

Interactive Discussion
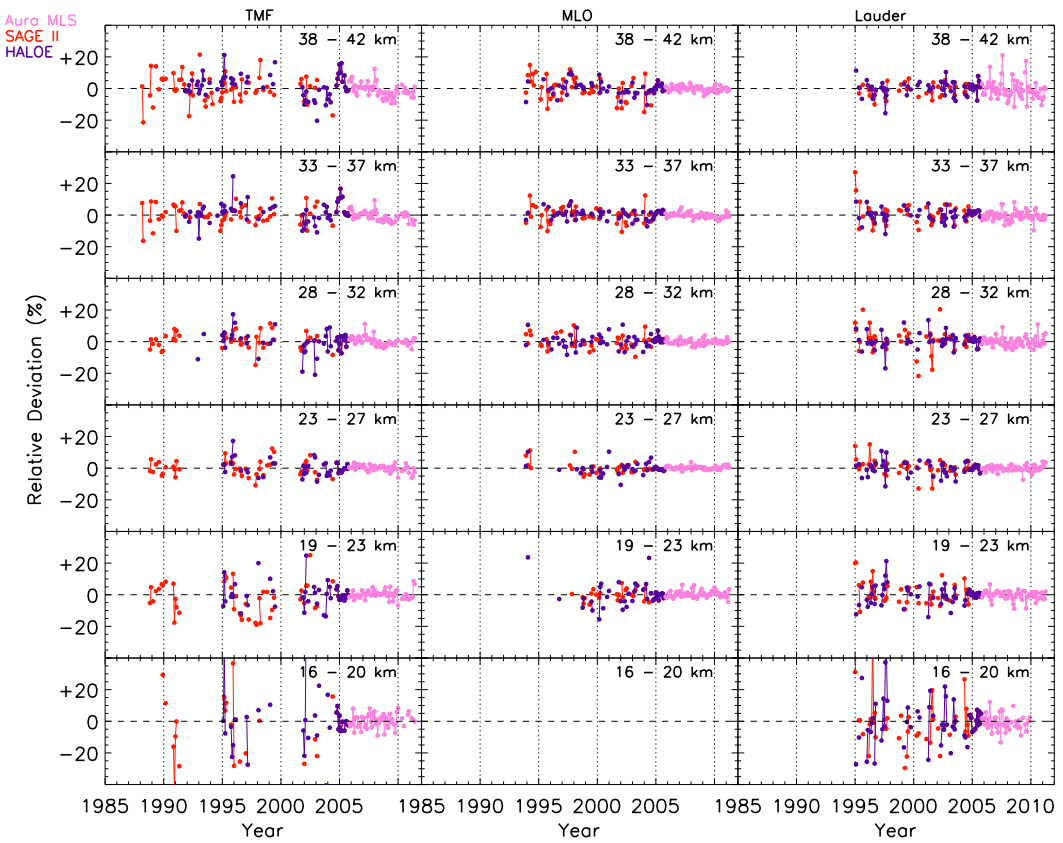
Fig. 9. Same as Fig. 8, but at TMF (left panel), MLO (middle panel) and Lauder (right panel).
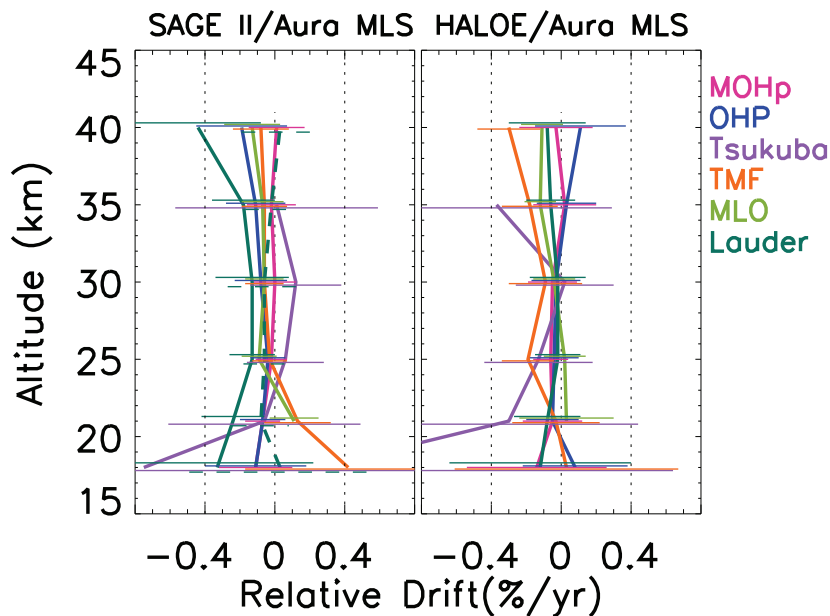
Fig. 10. The drifts evaluated from the combined time series of SAGE II/Aura MLS (left) and HALOE/Aura MLS (right) at various stations. The dashed line in the left panel represents the drift of SAGE II/Aura MLS at Lauder estimated after removing the first two measurements. The error bars represent twice the standard deviation of the slope. The dotted vertical lines represent 0 and $\pm 0.4\,\% \,\mathrm{yr}^{-1}$.